Applied Catalysis B: Environmental 186 (2016) 151–156

Contents lists available at ScienceDirect

Applied Catalysis B: Environmental

journal homepage: www.elsevier.com/locate/apcatb

On the performance of Pd and Rh catalysts over different supports in the hydrodechlorination of the MCPA herbicide

Elena Diaz[a,*], Angel F. Mohedano[a], Jose A. Casas[a], Cigdem Shalaby[b], Semih Eser[b], Juan J. Rodriguez[a]

[a] Sección de Ingeniería Química, Facultad de Ciencias, Universidad Autónoma de Madrid, Campus de Cantoblanco, 28049 Madrid, Spain
[b] Department of Energy and Mineral Engineering and EMS Energy Institute, The Pennsylvania State University, University Park 16801, USA

ARTICLE INFO

Article history:
Received 13 October 2015
Received in revised form
23 December 2015
Accepted 31 December 2015
Available online 6 January 2016

Keywords:
Hydrodechlorination
Pd supported catalysts
Rh supported catalysts
MCPA
Catalyst deactivation

ABSTRACT

Commercial and own-made Pd and Rh catalysts supported on alumina, zeolite Y (ZY) and two kinds of silica (Fumed Silica (FS) and SBA-15), were tested in the aqueous phase hydrodechlorination of the 4-chloro-2-methylphenoxyacetic acid (MCPA) herbicide. Pd catalysts showed higher activity than Rh and regarding the supports, the following sequence was found: Al_2O_3 > FS > ZY » SBA-15. The catalysts with metal particle sizes within the range of 3.1–3.7 nm, associated with M^{n+}/M° ratios between 0.7 and 1.7, showed higher activities. The most active catalysts of each series, the Al_2O_3-supported ones, showed a distribution of the metallic phase approaching an egg-shell configuration opposite to the rest. The Pd/Al_2O_3 catalyst, which was the most active, suffered a significant loss of activity upon the early stages on stream that could be ascribed to the formation of palladium chloride complexes as well as to deposition of species involved in the reaction.

© 2016 Elsevier B.V. All rights reserved.

1. Introduction

Catalytic hydrodechlorination (HDC) is an effective and environmentally friendly method for the transformation of organochlorinated water pollutants into species of much lower toxicity. So far, the development of good catalysts combining high activity and stability is crucial for the full-scale implementation of that emerging technology. Pd catalysts have shown a high activity in HDC reactions based on the high ability of this metal to promote the hydrogenolysis of CCl bonds, whereas other precious metals, like Rh, present also good expectations and have shown an interesting behavior in terms of further hydrogenation of the primary dechlorinated products [1,2]. The nature of the support is an important issue on the performance of those catalysts since it can affect to the dispersion of the active phase and to the ratio of zerovalent to electrodeficient metallic species, both important factors regarding the activity and stability [3–7].

So far the main inorganic support used in aqueous phase HDC catalysts has been alumina, followed by silica and zeolites, while activated carbon represents another type of support of different nature also used for that reaction. Activated carbon has been widely used as catalytic support due to both physical and chemical properties, being the main advantage its high surface area which favors a high dispersion of the active phase. However, its high and unspecific adsorption capacity may result in a rapid fouling of the catalyst. On the other hand, inorganic supports usually present lower adsorption capacity, with specific surface area values in the range of 100–200 m^2/g. Alumina has attracted much attention as catalyst support because of its three-dimensional interconnected pore system and its mechanical strength [8]. The cation exchange capacity of zeolites permits the easy introduction of the metal active phase, but its use as a high surface area microporous support for noble metals does not appear to offer any real advantage with respect to other mesoporous materials in aqueous-phase HDC. Important characteristics such as the pore size and hydrophobicity of zeolites can be modified varying the Si/Al ratio but the poisoning of the noble metal by HCl is not minimized by the zeolite support as it happens with Al_2O_3, though this can be improved with the zeolite Y [8–10]. The main property of silica as catalytic support lies on its high stability in hydrotreatment processes as well as the formation of smaller and stable particles of active phase [11].

There are several studies in the literature on aqueous phase HDC analyzing the activities of catalysts supported on inorganic oxides. In general, good results have been achieved with Pd/Al_2O_3 [1,3,12–15], Pd/SiO_2 [16,17] and Pd/zeolites catalysts [9]. On the other hand, the use of Rh on inorganic oxides catalysts is less

* Corresponding author. Fax: +34 914973516.
E-mail address: elena.diaz@uam.es (E. Diaz).

http://dx.doi.org/10.1016/j.apcatb.2015.12.054
0926-3373/© 2016 Elsevier B.V. All rights reserved.

widespread, although fairly good results have been reported in the HDC of chlorophenols [1,7].

In this work, we analyze the performance of several commercial and own-made Pd and Rh catalysts supported on alumina, zeolites and silica (fumed silica and an ordered mesoporous silica, SBA-15) in aqueous-phase HDC at ambient-like conditions using 4-chloro-2-methylphenoxyacetic acid (MCPA) as target compound. This is one of the most widely used herbicides for agricultural and residential applications in US, Europe and Japan [18]. The use of herbicides for intense agricultural practices or their release as a consequence of cleaning operations (containers, pipelines, equipments) can contribute to the contamination of surface water bodies and groundwater. MCPA is characterized as toxic and persistent, and is included in the list of priority pollutants of the European Union and classified by EPA as a potential groundwater pollutant. Different techniques have been proposed to remove MCPA from water, such as adsorption [19–21], advanced oxidation processes (AOPs), including the Fenton reaction [22,23], heterogeneous photocatalysis [24,25], ozonization [26] and nonconventional biological solutions or hybrid configurations (AOPs + biological treatment) [27,28]. HDC can transform conveniently this kind of pollutants to non-chlorinated species allowing easier subsequent biological degradation.

In the current work, the activity of the catalysts tested has been related with some of their main characteristics, like surface area, metal dispersion and the oxidation state of the metal species. Since the stability is a critical issue regarding potential application, the performance of the most active catalyst has been tested in a long-term experiment (100 h). The evolution of the catalytic activity upon time on stream has been analyzed on the basis of the fresh and used catalyst characterization.

2. Materials and methods

2.1. Catalyst description and characterization

The Pd/Al_2O_3 and Rh/Al_2O_3 catalysts were supplied by BASF as egg-shell spheres with a diameter of 2.4–4 mm and a metal loading of 0.5% wt [1]. Monometallic palladium and rhodium catalysts were synthesized by incipient wetness impregnation, using a commercial fumed silica (CAB-O-SIL® M-5, CABOT), a SBA-15 silica and a zeolite Y as supports. SBA-15 was prepared according to the method described elsewhere [29–31]. Typically, a homogeneous mixture composed of triblock copolymer Pluronic of P123 (EO20PO70EO20, MW = 5800, Aldrich) and tetraethyl orthosilicate (TEOS) in hydrochloric acid was stirred at 40 °C for 20 h and then treated at 100 °C for 24 h. The solid product was filtered and washed with plenty of water, dried in an oven at 100 °C, and subsequently calcined at 550 °C for 6 h under air flow (100 N mL/min). Zeolite Y (SiO_2/Al_2O_3 molar ratio: 30) was obtained from Zeolyst International (formerly PQ Corporation) and calcined in air flow (~60 N mL/min) for 4 h at 450 °C which was reached at 1.5 °C/min heating rate. The K^+ exchanged zeolite Y support was prepared by ion exchange of zeolite Y with 0.4 M aqueous solution of potassium chloride (KCl, Aldrich, 99.0%). Then, it was washed with deionized water, oven dried at 100 °C and calcined at 450 °C for 4 h.

The impregnation solutions consisted in $PdCl_2$ and $RhCl_3$ (Sigma–Aldrich) dissolved in 0.1 N HCl aqueous solution. Impregnation was followed by drying at room temperature for 2 h and overnight at 60 °C. Finally, the catalysts were calcined at 200 °C for 3 h in air atmosphere. The samples were reduced at 150 °C under continuous H_2 flow (50 N mL/min) for 1.5 h before the HDC experiments.

The BET surface area of the catalysts was calculated from the 77 K N_2 adsorption–desorption isotherms obtained in a Tristar 3020 Micromeritics apparatus. Approximately 0.15 g of sample were used in each test. The samples were placed in a glass container and degassed at 150 °C and 75 mTorr residual pressure for 12–16 h prior to the adsorption measurements using a Micromeritics sample degas system (VacPrep 061). The metal content was determined by inductively coupled plasma-mass spectroscopy (ICP-MS) in a PerkinElmer model Elan 6000 Sciex system that was equipped with an autosampler (PerkinElmer model AS 91). Metallic surface concentrations were determined by X-ray photoelectron spectroscopy (XPS) with a VG Escalab 200R spectrometer equipped with a hemispherical electron analyzer (pass energy of 20 eV) and a Mg KR ($h\nu$ = 1254.6 eV) X-ray source, powered at 120 W. Metal dispersion and the average metal particle size of the catalysts were determined from CO chemisorption at room temperature in a Micromeritics Chemisorb 2750 automated system equipped with ChemiSoft TPx software. The metal particle size ($\bar{d_i}$ (nm)) was calculated from Eq. (1) that assumes the spherical shape of the metal particles [32]:

$$\bar{d_i} = \frac{6 \times 10^9 \times V_M}{A_M \times D(\%)} \quad (1)$$

where V_M is the bulk atomic volume of the metal (cm^3), A_M is the shade atomic area (cm^2) and D the metal dispersion (%). Before the chemisorption measurements, the samples were reduced in H_2 flow (30 N mL/min) at 150 °C for 2 h and then cooled down to ambient temperature in He flow (30 N mL/min). To obtain the Pd and Rh dispersion the stoichiometry of the CO adsorption over the Pd and Rh atoms was assumed to be 1:1 [33]. Thermogravimetric analyses were performed in a Mettler SDTA851e model TGA apparatus under 50 N mL/min continuous air flow. A weighted amount (approaching 20 mg) of sample was heated at 2 °C/min up to 110 °C, temperature that was maintained for 1 h in order to remove the moisture of the samples, which were subsequently heated at 2 °C/min up to 800 °C.

2.2. Hydrodechlorination experiments

The HDC runs were performed in a stainless steel stirred tank (100 mL) from Autoclave Engineers, provided with temperature, pressure and gas flow control. 80 mL of a 0.8 mM aqueous solution of MCPA (>99.0% purity Sigma–Aldrich) were placed in the reactor and hydrogen was continuously fed at a flow rate of 25 N mL/min. A temperature of 30 °C, pressure of 1.4 bar, a catalyst loading of 0.25 g/L and a stirring velocity of 600 rpm were always used. The catalyst particle size was lower than 100 μm. Constant gas flow rate and reactor pressure were maintained by means of a mass flow controller and a back-pressure control valve, respectively. The reactor was heated up to the working temperature, this being measured and controlled by a thermocouple in the liquid phase. Liquid samples were periodically withdrawn from the reactor and the catalyst was separated by filtration using a PTFE filter of 0.2 μm pore size.

A long-term experiment (100 h), to evaluate the stability of the most active catalyst, was carried out in a continuous stirred basket tank reactor (Carberry Spinning Catalyst Basket) from Autoclave Engineers at 30 °C, 1 bar and a stirring velocity of 600 rpm. MCPA aqueous solution (0.8 mM, 4 mL/min) and hydrogen (50 NmL/min) were continuously fed to the reactor. A mass of 0.5 g of catalyst (spherical particles of 2.4–2.8 mm), was load into the basket, being the space-time fixed at 2.95 kg_{cat} h/mol_{MCPA}. The data reproducibility was better than ±5%.

The extent of the reaction was determined from the analysis of the liquid phase. The concentration of MCPA and its dechlorination product (2-methylphenoxyacetic acid (MPA)) were quantified by HPLC (Varian Prostar 325) with a UV detector at 280 nm using a C18 column as stationary phase (Valco Microsorb-MW 100-5C18) and a mixture of acetonitrile and 0.1% aqueous acetic acid as mobile phase at 0.5 mL/min. Chloride ion was analyzed by ionic chromatogra-

Table 1
Characterization of the catalysts.

Catalyst	Support	A_{BET} (m^2/g)	V_{pore} (cm^3/g)	d_{pore} (nm)	M_{bulk} (wt.%)	M_{XPS} (wt.%)	M_{XPS}/M_{bulk}	M^{n+}/M°	D (%)	$\bar{d}$ (nm)
Pd/Al_2O_3	γ-Al_2O_3	94	0.36	13	0.47	0.95	2.02	1	34	3.3
Pd/FS	Fumed silica	200	0.87	14	0.45	0.31	0.69	0.69	30	3.7
Pd/SBA-15	SBA-15	720	1.12	6	0.48	0.42	0.88	0.27	10	11.2
Pd/ZY	K^+ exchanged zeolite Y	772	0.57	2.5	0.49	0.20	0.41	0.50	49	2.3
Rh/Al_2O_3	γ-Al_2O_3	110	0.38	13	0.51	0.92	1.80	1.7	35	3.1
Rh/FS	Fumed silica	206	0.95	17	0.48	0.20	0.42	0.67	30	3.7
Rh/SBA-15	SBA-15	733	1.10	5.5	0.47	0.30	0.64	1.1	17	6.5
Rh/ZY	K^+ exchanged zeolite Y	640	0.47	2.9	0.50	0.31	0.62	0.61	67	1.6
Pd/Al_2O_3-Used	γ-Al_2O_3	84	0.35	12	0.45	0.70	1.56	0.43	28	4.0

M: metal (Pd or Rh); *D*: metal dispersion. Used: catalyst after being used in a long term HDC run.

phy (Metrohm 790 Personal IC). Analysis of Pd in the liquid stream exiting the reactor along long-term experiment was carried out by total reflection X-ray fluorescence (TXRF) with a TXRF EXTRA II spectrometer.

3. Results and discussion

3.1. Characterization of the catalysts

Table 1 summarizes the characterization of the catalysts. The N_2 adsorption–desorption isotherms were typical of mesoporous solids, except for the catalysts using ZY as support, which showed a significant contribution of microporosity (micropore volume: Pd/ZY = 0.32 cm^3/g; Rh/ZY = 0.25 cm^3/g). Regarding the mesoporous materials, the catalysts supported on SBA-15 had a more developed porosity as indicate the higher values of surface area and total pore volume. The Al_2O_3- and FS-supported catalysts had quite similar mean pore size (13–17 nm), whereas in the case of SBA-15 that dimension was much smaller.

The chemical analyses confirmed that the bulk metal content approaches closely the 0.5% wt nominal value. With regard to the outermost surface metal content determined by XPS, the catalysts supported on alumina yielded around double the bulk concentration. This indicates that the metallic particles must be predominantly located in the external surface, giving rise to an egg-shell type distribution, in this case with a fairly good dispersion. The opposite seems to occur with the silica- and zeolite-supported catalysts whereas for the SBA-15 ones a more homogeneous distribution appears more likely, most in particular in the case of the Pd catalyst.

Deconvolution of the core-level spectra of *3d* orbital of each metal (Fig. S1 of Supplementary information) evidenced the existence of zerovalent and electrodeficient species for Pd and Rh. In the case of Pd catalysts, two main bands centered at binding energy values of 335.5 and 337.0 eV were observed for Pd $3d_{5/2}$, which can be attributed to Pd° and Pd^{n+}, respectively. The Rh $3d_{5/2}$ peak lying around 307.2 eV can be attributed to Rh°, while the Rh $3d_{5/2}$ peak located around 309.5 eV is related to Rh^{n+}. The values of the electrodeficient to zerovalent metal ratio (M^{n+}/M°) are included in Table 1. The zerovalent is clearly the prevailing species except for the alumina-supported catalysts and the Rh/SBA-15 one.

The metal dispersion values were significantly higher for the catalysts supported on ZY, with average values of metal particle size lower than 2.5 nm, while the poorest dispersion was associated with the SBA-15-supported catalysts, yielding average metal particle sizes of 11.2 and 6.5 nm for the Pd and Rh catalysts, respectively. These metal particle sizes are within the range reported in the literature and are related to the parallel and poorly interconnected mesopores that characterize that material [34]. The average metal particle sizes of the Al_2O_3- and FS-supported catalysts were fairly close (3.1–3.7 nm). The existence of some dependence between the metal particle size and the ratio of electrodeficient to zerovalent metallic species has been analyzed by some authors without a conclusive agreement [35,36]. Baeza et al. [36] found that unsupported Pd nanoparticles within the range of 2.7–4.2 nm showed the lowest Pd^{n+}/Pd° ratios (0.35–0.67) and in the case of Rh the lowest Rh^{n+}/Rh° ratio (0.56–0.72) corresponded to nanoparticles sized between 2.3 and 3.0 nm [7]. In the current work we could not establish a conclusive connection between those two characteristics.

Table 2
Values of the apparent rate constants ($L \times (g_{cat}\ min)^{-1}$) and TOF ($min^{-1}$) for HDC of MCPA with several Pd and Rh catalysts.

Catalyst	k ($L \times (g_{cat}\ min)^{-1}$)	r^2	TOF (min^{-1})
Pd/Al_2O_3	0.63 ± 0.024	0.993	15
Pd/FS	0.24 ± 0.004	0.997	13
Pd/SBA-15	0.06 ± 0.004	0.984	12
Pd/ZY	0.18 ± 0.008	0.991	4.4
Rh/Al_2O_3	0.14 ± 0.004	0.994	5.0
Rh/FS	0.10 ± 0.004	0.990	5.1
Rh/SBA-15	0.01 ± 0.004	0.951	1.8
Rh/ZY	0.09 ± 0.004	0.999	2.0

3.2. Catalytic activity

With all the catalysts tested, the HDC of MCPA gave rise to the formation of 2-methylphenoxyacetic acid (MPA) and hydrogen chloride. The measured concentrations of MCPA and MPA represented more than 98% of the initial C in all the samples analyzed along the reaction time covered in the experiment (1 h). Therefore, further hydrogenation of MPA can be assumed almost negligible if any.

The evolution of MCPA conversion upon reaction time is shown in Fig. 1. The Al_2O_3-supported catalysts showed the best results for both metals and Pd yielded significantly higher dechlorination rates than Rh, allowing complete dechlorination at the end of the 1 h reaction time of the experiments except in the case of the SBA-15-supported catalyst, which showed fairly poorer activity than the rest for both, Pd and Rh. No complete conversion of MCPA was accomplished for any Rh catalyst in 1 h reaction time. These results are in agreement with the well-known high ability of Pd for the hydrogenolysis of the C—Cl bond.

A simple pseudo-first-order rate equation was checked to describe the conversion of MCPA into MPA, where the concentration of hydrogen can be considered constant. Table 2 collects the values of the rate constant as well as those of the correlation coefficient. The existence of external mass transfer limitations is discarded in our experimental conditions, as demonstrated in previous studies [1], whereas the effectiveness factors (η), determined from the estimation of Thiele modulus [37] were always higher than 0.99, because the MCPA HDC reaction proceeds at relatively low rate. Therefore, internal diffusion limitation can be discarded. From the results so far the following sequence can be established relative to the activity of the catalysts regarding the supports: Al_2O_3 > FS > ZY » SBA-15. According to this, the supports

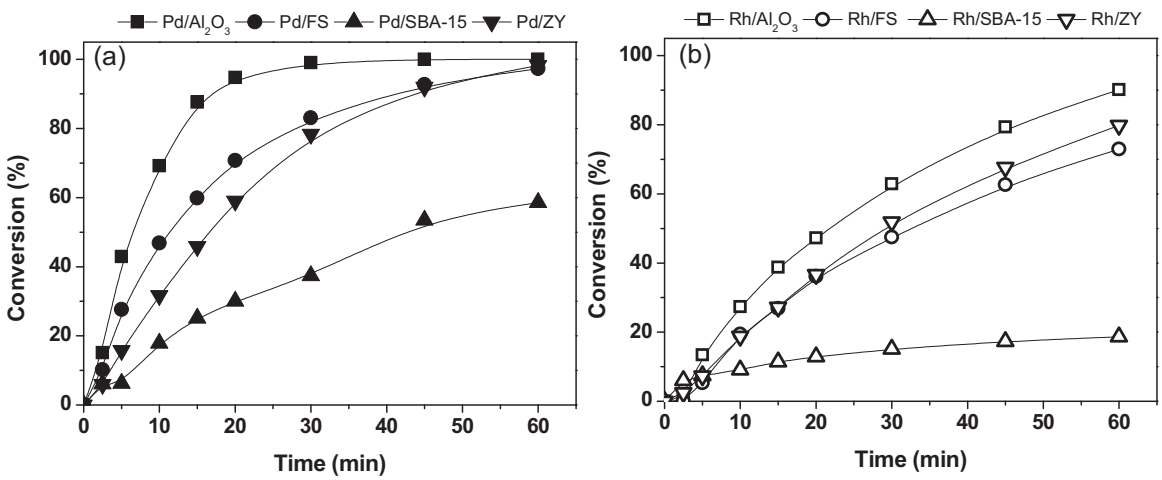

Fig. 1. HDC of MCPA with the Pd (a) and Rh (b) catalysts tested.

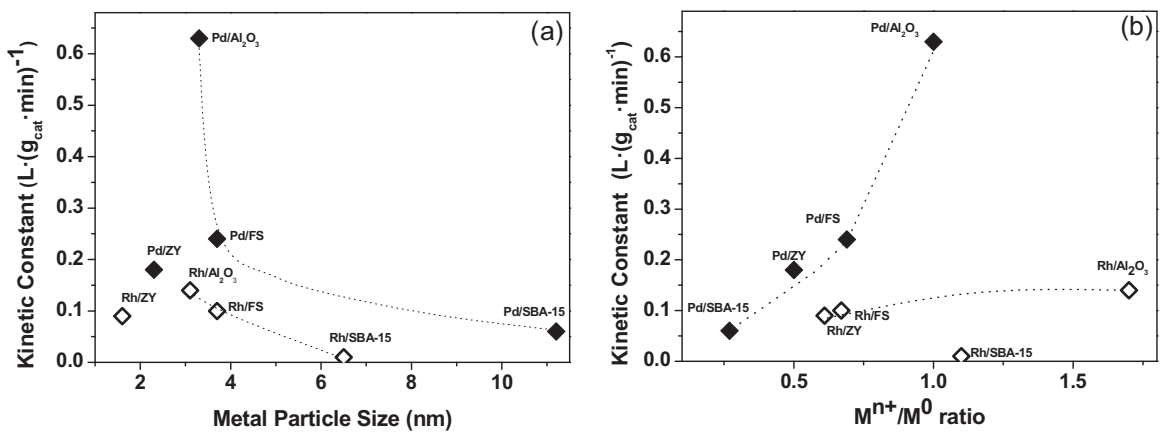

Fig. 2. Values of the apparent rate constant versus average metal particle size (a) and M^{n+}/M° ratio (b).

with a mesoporous structure ($d_{pore} \geq 13$ nm) seem to be better for this reaction than those with a narrower pore sizes. In terms of TOF, there are only small differences between the specific activity exhibited, by the Pd catalysts, except the zeolite-supported one. The Rh catalysts yielded lower TOF values, being quite similar those of Rh/Al_2O_3 and Rh/FS, higher than the zeolite and SBA-15 supported ones.

Fig. 2 shows the dependence of the kinetic constant on the metal particle size (a) and on the M^{n+}/M° ratio (b). The differences observed among the Pd catalysts are much more significant than for the Rh ones. Nevertheless, in both cases, the rate constant shows a maximum centered around 3.5 nm. That maximum is fairly sharp in the Pd series suggesting some additional specific effect of the Al_2O_3 support although that situation is not observed in the case of Rh. In spite of the fact that the metallic dispersion, and consequently the metal particle size, have been identified as critical to the catalytic activity in HDC, there is no a conclusive agreement on whether this reaction is structure sensitive. Some studies have reported higher activities for smaller metal particle (<5 nm) [4] or have established a metal particle within 3–4 nm as the optimum [2]. Baeza et al. [7,36], observed that decreasing the particle size increased the catalytic activity of unsupported Pd and Rh nanoparticles in the HDC of 4-chlorophenol, suggesting 2.7–2.8 nm as the optimum size. However, contradictory results have been also found in the literature and the highest values of the rate constant have been associated with largest Pd particles (>30 nm) in the HDC of trichloroethylene with Pd on different carbon materials [38]. To gain some knowledge

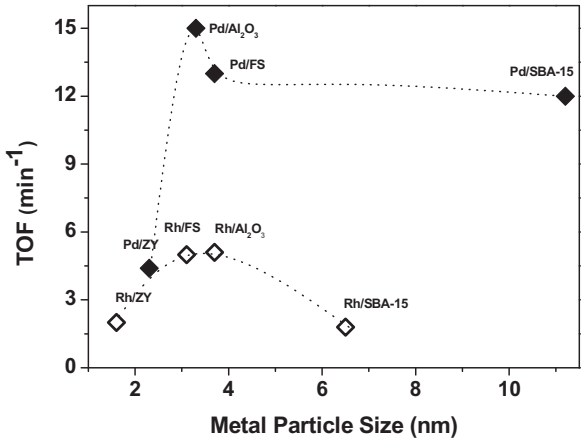

Fig. 3. TOF values versus average metal particle size.

on the structure sensitiveness of the HDC reaction, Fig. 3 represents the TOF values versus the average metal particle size. As can be seen, the catalysts with metal particle size between 3.1 and 3.7 nm show the highest TOF values in both metal series, whereas those with the smallest metal particles (<2.3 nm) showed poorer specific activity. The existence of that optimum range of metal particle size appears clearer in the case of Rh whereas for Pd only a small decrease of TOF was observed above the aforementioned range.

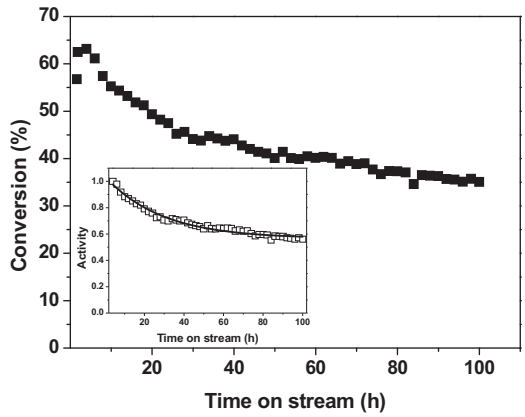

Fig. 4. MCPA conversion versus time on stream with the Pd/Al_2O_3 catalyst and fitting of the experimental results to the deactivation rate equation (box curve).

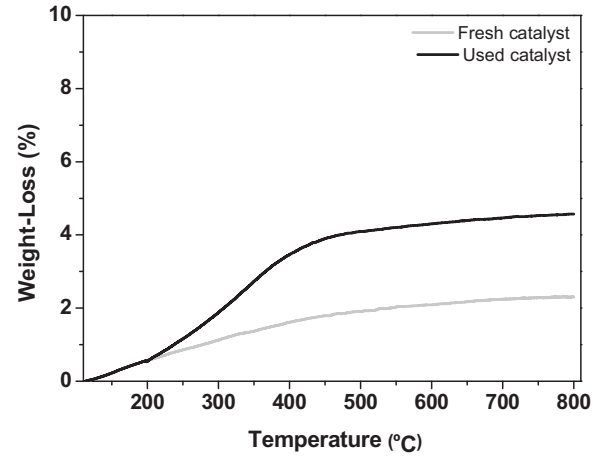

Fig. 5. TGA profiles in air atmosphere of the fresh and used Pd/Al_2O_3 catalyst.

The low activity of zeolite-supported catalysts can be associated with their prevailing microporous structure. In spite of the fact that those catalysts presented the highest values of dispersion, the small metal particles can be placed in less accessible positions. The ratio of bulk to external (XPS) metal concentration of the Pd/ZY and Rh/ZY catalysts (Table 1) suggests that the metallic phase is mostly distributed in the inner part of the catalyst particles. Schut et al. [9] reported that in the HDC of 1,2-dichlorobenzene with Pd on zeolites catalysts, the reaction rate increased with increasing the average pore size.

Several studies have demonstrated that both electro-deficient and metallic species are required for the HDC reaction [3,5,38,39]. The results of Fig. 2b show a significant increase of the apparent rate constant with the M^{n+}/M° ratio in the case of the Pd catalyst. A value of that ratio around 1 seems to be optimum for this reaction [3,36]. With the Rh catalysts the possible effect of the M^{n+}/M° ratio is much less pronounced although again increasing that ratio increases the rate constant, except for the SBA-15-supported catalyst. Further evidences would be needed before establishing a conclusive approach about the influence of the M^{n+}/M° ratio on the rate of HDC.

Regarding the distribution of the metallic phase onto the catalyst particles, an egg-shell approach seems to favour the reaction rate since, as indicated before, that is the case of the Al_2O_3-supported catalysts, the most active of each series, whereas a more homogeneous or even egg-yolk distribution appears more likely for the rest according with the bulk XPS metal concentrations (see Table 1).

3.3. Stability of the Pd/Al_2O_3 catalyst

A long-term experiment was performed with the most active catalyst, Pd/Al_2O_3. The performance of the catalyst upon 100 h on stream is shown in Fig. 4 in terms of the evolution of MCPA conversion. The carbon balance was always closed around 98%. At the working space-time (2.95 kg_{cat} h/mol_{MCPA}) 65% conversion was maintained for around 5 h and then a continuous decay of activity was observed, more significant within the range of 10–30 h on stream. Beyond that time a slow evolution towards a residual activity appears to be the trend.

A well known equation was used to describe the rate of deactivation (Eq. (2)), which takes into account the residual activity of the catalysts (a_∞). This equation has been used in previous studies of catalyst deactivation in HDC reactions [5,6,40].

$$-\frac{da}{dt} = k_d \times (a - a_\infty) \quad (2)$$

where k_d is the deactivation kinetic constant (h^{-1}) and a is the catalyst activity (dimensionless, 0–1) defined as the ratio between the reaction rate at t time on stream and the initial. The results are depicted in Fig. 4, where it can be seen the good fitting of the experimental and predicted results. The values obtained for the deactivation constant and the residual activity were $0.041 \pm 0.002\ h^{-1}$ and 0.587 ± 0.006, respectively. Previous results on the HDC of MCPA with a Pd on activated carbon catalyst showed a progressive and severe deactivation upon time on stream attributed to fouling of the catalyst by deposition of reaction species [40,41]. In this case, the loss of activity of the Pd/Al_2O_3 catalyst occurred mostly within the early stages on stream then followed by a significantly slower deactivation.

To learn on the causes of deactivation of the Pd/Al_2O_3 catalyst, it was characterized after the 100 h on stream. The results are included in Table 1. Pd was analyzed in the reactor effluent at different times and metal leaching can be considered negligible. Moreover, no significant differences were found in the content of bulk Pd in the fresh and the used catalyst, so that it can be discarded as a cause of deactivation. The occurrence of a moderate fouling of the catalyst surface is consistent with the decrease of surface area together with the analyzed carbon content of the used catalyst (1.7%). The TGA curves of the fresh and used catalyst in air atmosphere are depicted in Fig. 5. The used catalyst showed a significantly higher weight loss within the 200–500 °C range which can be attributed to the burn-off of organic species on the catalyst surface.

A significant difference between the fresh and used catalyst refers to the surface Pd^{n+}/Pd° ratio and Pd concentration determined by XPS. This last is also consistent with a partial coverage of the surface catalysts by adsorbed species. Regarding to the decrease of Pd^{n+}/Pd° ratio (Fig. S2 of Supplementary information), it can be partially explained by the reduction of electrodeficient to zerovalent palladium under the hydrogen-rich environment of the reaction. Nevertheless, the important decrease of the Pd^{n+}/Pd° ratio at the mild operating temperature may be due to some other cause. In that sense, chlorinated species could interact with electrodeficient palladium through the formation of palladium–chlorine complexes, thus decreasing the number of active centers available for the reaction, which is also consistent with the increment of Cl content on the catalyst surface detected by XPS (0.57% wt in the used catalyst versus 0.19% wt in the fresh one). This cause of deactivation of Pd/Al_2O_3 catalysts has been suggested in the aqueous phase HDC of trichloroethylene and 4-chlorophenol [5,6]. The used catalyst yielded a somewhat lower dispersion than the fresh one. Sintering of Pd particles is unlikely

under the ambient-like working temperature (30 °C). Therefore, that decrease of dispersion must be due to the coverage of some palladium sites, giving rise to a decreased CO chemisorption.

4. Conclusions

Pd and Rh catalysts using different inorganic supports have been evaluated in the aqueous phase HDC of MCPA. The Pd catalysts were more active than Rh ones and regarding to the supports, the following sequence was established: Al_2O_3 > FS > ZY » SBA-15 indicating that a mesoporous structure with a mean pore size within the range of 13–17 nm appears the most favorable. Regarding to the metal particle size, the catalysts with small metal particles yielded higher reaction rates with a maximum at ~3.5 nm. Increasing the M^{n+}/M° ratio (determined by XPS) up to around 1 seems to favor the HDC rate although a conclusive response can not be given from the results so far. Distribution of the metallic active phase on the catalyst surface approaching egg-shell configuration seems also to be more favourable.

The evaluation of the stability of the most active catalyst, the Pd/Al_2O_3 one, showed an appreciable loss of activity mostly upon the early stages then followed by a slower deactivation driving to a residual activity close to 60% of the initial. The characterization of the fresh and used catalyst allows concluding that fouling of the catalyst surface by the deposition of species involved in the reaction must be the main cause of deactivation. That may include the formation of Pd–chlorine complexes.

Acknowledgements

We gratefully appreciate financial support through REMTAVARES S-2013/MAE-2716 and CTQ2013-41963-R from the Consejería de Educación of the CM and the Spanish MICINN, respectively. E. Diaz and A.F. Mohedano would like to thank their grants from the Spanish Ministerio de Educacion through the Programa Nacional de Movilidad de Recursos Humanos del Plan Nacional de I-D + i 2008–2011. Moreover, the authors thank to the "Servicios de Análisis y Caracterización de Sólidos y Superficies de la Universidad de Extremadura" for assistance in the XPS analyses.

Appendix A. Supplementary data

Supplementary data associated with this article can be found, in the online version, at http://dx.doi.org/10.1016/j.apcatb.2015.12.054.

References

[1] E. Diaz, J.A. Casas, A.F. Mohedano, L. Calvo, M.A. Gilarranz, J.J. Rodriguez, Ind. Eng. Chem. Res. 47 (2008) 3840–3846.
[2] E. Diaz, A.F. Mohedano, J.A. Casas, L. Calvo, M.A. Gilarranz, J.J. Rodriguez, Appl. Catal. B 106 (2011) 469–475.
[3] L.M. Gómez-Sainero, X.L. Seoane, J.L.G. Fierro, A. Arcoya, J. Catal. 209 (2002) 279–288.
[4] S. Gomez-Quero, F. Cardenas-Lizana, M.A. Keane, Chem. Eng. J. 166 (2011) 1044–1051.
[5] S. Ordonez, B.P. Vivas, F.V. Diez, Appl. Catal. B 95 (2010) 288–296.
[6] Z.M. de Pedro, E. Diaz, A.F. Mohedano, J.A. Casas, J.J. Rodriguez, Appl. Catal. B 103 (2011) 128–135.
[7] J.A. Baeza, L. Calvo, M.A. Gilarranz, J.J. Rodriguez, Chem. Eng. J. 240 (2014) 271–280.
[8] S.C. Shekhar, J.K. Murthy, P.K. Rao, K.S.R. Rao, Appl. Catal. A 271 (2004) 95–101.
[9] C. Schuth, S. Disser, F. Schuth, M. Reinhard, Appl. Catal. B 28 (2000) 147–152.
[10] R.F. Howe, Appl. Catal. A 271 (2004) 3–11.
[11] J.A. Cecilia, A. Infantes-Molina, E. Rodriguez-Castellon, A. Jimenez-Lopez, J. Hazard. Mater. 260 (2013) 167–175.
[12] H.M. Roy, C.M. Wai, T. Yuan, J.K. Kim, W.D. Marshall, Appl. Catal. A 271 (2004) 137–143.
[13] G. Yuan, M.A. Keane, Appl. Catal. B 52 (2004) 301–314.
[14] M.O. Nutt, J.B. Hughes, M.S. Wong, Environ. Sci. Technol. 39 (2005) 1346–1353.
[15] E. Diaz, J.A. Casas, A.F. Mohedano, L. Calvo, M.A. Gilarranz, J.J. Rodriguez, Ind. Eng. Chem. Res. 48 (2009) 3351–3358.
[16] I. Witonska, A. Krolak, S. Karski, J. Mol. Catal. A 331 (2010) 21–28.
[17] S.W. Zhou, X. Jin, F.F. Sun, H. Zhou, C.Y. Yang, C.H. Xia, Water Sci. Technol. 65 (2012) 780–786.
[18] M. Kubota, M. Hayashi, H. Matsuda, H.J. Serizawa, J. Mater. Cycles Waste Manage. 14 (2012) 132–138.
[19] A. De Martino, M. Iorio, B. Xing, R. Capasso, RSC Adv. 2 (2012) 5693–5700.
[20] D. Werner, J.A. Garrat, G. Pigott, J. Soils Sediment 13 (2013) 129–139.
[21] K. Kusmierek, M. Sankowska, A. Swiatkowski, Desalin. Water Treat. 52 (2014) 178–183.
[22] E. Brillas, B. Boye, I. Sirés, J.A. Garrido, R.M. Rodriguez, C. Arias, P. Cabot, C. Comninellis, Electrochim. Acta 49 (2004) 4487–4496.
[23] S. Garcia-Segura, L.C. Almeida, N. Bocchi, E. Brillas, J. Hazard. Mater. 194 (2011) 109–118.
[24] K. Djebbar, A. Zertal, T. Sehil, Environ. Technol. 27 (2006) 1191–1197.
[25] E. Diaz, M. Cebrian, A. Bahamonde, M. Faraldos, A.F. Mohedano, J.A. Casas, J.J. Rodriguez, Catal. Today (2015), http://dx.doi.org/10.1016/j.cattod.2015.08.013.
[26] R.R. Solís, F.J. Rivas, J.L. Pérez-Bote, O. Gimeno, J. Taiwan Inst. Chem. E 46 (2015) 125–131.
[27] I. Oller, S. Malato, J.A. Sánchez-Pérez, Sci. Total Environ. 409 (2011) 4141–4166.
[28] S. Sanchis, A.M. Polo, M. Tobajas, J.J. Rodriguez, A.F. Mohedano, Chemosphere 93 (2013) 115–122.
[29] W. Wang, Q. Zhang, S. Yang, Y. Wang, J. Phys. Chem. B 109 (2005) 23500–23508.
[30] D. Zhao, J. Feng, Q. Huo, N. Melosh, G.H. Fredrickson, B.F. Chmelka, G.D. Stucky, Science 279 (1998) 548–552.
[31] C. Sentorun-Shalaby, S.K. Saha, X. Ma, C. Song, Appl. Catal. B 101 (2011) 718–726.
[32] M.A. Vannice, Catalyst characterization, in: M.A. Vannice, W.H. Joyce (Eds.), Kinetics of Catalytic Reactions, Springer, New York, 2005, pp. 14–37.
[33] S.H. Ali, J.G. Goodwin, J. Catal. 176 (1998) 3–13.
[34] G. Prieto, A. Martinez, R. Murciano, M.A. Arribas, Appl. Catal. A 367 (2009) 146–156.
[35] F. Chen, Z. Zong, X. Xu, J. Luo, J. Mater. Sci. 40 (2005) 1517–1519.
[36] J.A. Baeza, L. Calvo, M.A. Gilarranz, A.F. Mohedano, J.A. Casas, J.J. Rodriguez, J. Catal. 293 (2012) 85–93.
[37] H.H. Lee, Heterogeneous Reactor Design, Butterworth Publishers, Boston, 1985.
[38] E. Diaz, L. Faba, S. Ordonez, Appl. Catal. B 104 (2011) 415–417.
[39] M.A. Aramendia, R. Burch, I.M. Garcia, A. Marinas, J.M. Marinas, B.W.L. Southward, F.J. Urbano, Appl. Catal. B 31 (2001) 163–171.
[40] E. Diaz, A.F. Mohedano, J.A. Casas, L. Calvo, M.A. Gilarranz, J.J. Rodriguez, Catal. Today 241 (2015) 86–91.
[41] E. Diaz, A.F. Mohedano, J.A. Casas, J.J. Rodriguez, Appl. Catal. B 181 (2016) 429–435.